ACS OMEGA

http://pubs.acs.org/journal/acsodf

Article

Silica-Carbonate of Ba(II) and Fe^{2+}/Fe^{3+} Complex as Study Models to Understand Prebiotic Chemistry

Selene R. Islas and Mayra Cuéllar-Cruz*

Cite This: *ACS Omega* 2021, 6, 35629−35640

Read Online

ACCESS | Metrics & More | Article Recommendations | Supporting Information

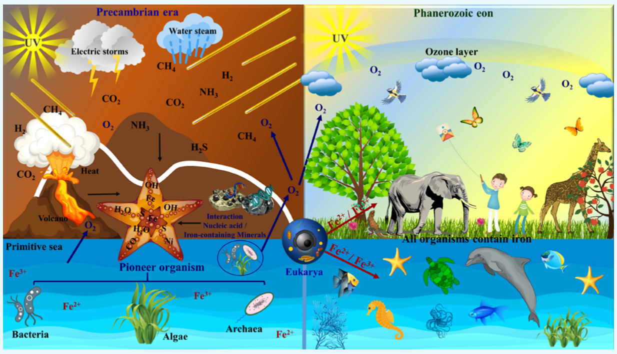

ABSTRACT: The Precambrian era is called the first stage of the Earth history and is considered the longest stage in the geological time scale. Despite its duration, several of its environmental and chemical characteristics are still being studied. It is an era of special relevance not only for its duration but also because it is when a set of conditions gave rise to the first organism. This pioneer organism has been proposed to have been formed by a mineral and an organic part. A chemical element suggested to have been part of the structure of this cell is iron. However, what special characteristic does iron have with respect to other chemical elements to be proposed as part of this first cell? To answer this and other questions, it is indispensable to have a model that will allow extrapolating the first chemical structures of the pioneer organism formed in the Precambrian. In this context, for several decades, in vitro structures chemically formed by silica-carbonates have been synthetized, called biomorphs, because they could emulate living organisms and might resemble primitive organisms. It has been inferred that because biomorphs form structures with characteristic morphologies, they could resemble the microfossils found in the cherts of the Precambrian. Aiming at providing some insight on how iron contributed to the formation of the chemical structures of the primitive organism, we evaluated how iron contributes to the morphology and chemical−crystalline structure during the synthesis of these compounds under different conditions found in the primitive atmosphere. Experimentally, synthesis of biomorphs was performed at four different atmospheric conditions including UV light, nonionizing microwave radiation (NIR-mw), water steam (WS), and CO_2 in the presence of Fe^{2+}, Fe^{3+}, and Fe^{2+}/Fe^{3+}, obtaining 48 different conditions. The produced biomorphs were observed under scanning electron microscopy (SEM). Afterward, their chemical composition and crystalline structure were analyzed through Raman and IR spectroscopy.

1. INTRODUCTION

The Precambrian era is the most extensive geological era because it goes from the creation of Earth until the Cambrian explosion. During this time, relevant events happened related to the creation of the Earth, including the first chemical reactions that gave origin to the primitive organism and, consequently, to life. Evidence of life in the Precambrian has been reported in geological sediments of different ages of that era.[1−3] It has been documented that Precambrian sediments contain organic and inorganic compounds coming from microfossils and minerals found in that epoch, a fact that will allow understanding the origin and evolution of life on Earth.[2,4,5] Stromatolites are laminated or stratified structures formed by sediments and minerals from which microfossils and organic compounds originated by the degradation of other fossils that existed in the Precambrian era.[2,6−9] Among the organic compounds that have been identified in the different materials that constitute the Precambrian sediments, such as microfossils, stromatolites, and cherts (biogenic cherts are formed by radiolarians, diatoms, and sponge spicules), are lipids, aliphatic hydrocarbons, isoprenoid alkanes, fatty acids, ethers, ketones, carbon isotopic ratios, porphyrins, and amino acids.[1,6,10−12] Primitive minerals existing in the Precambrian era were formed by chemical elements like nitrogen, oxygen, sodium, silicon, calcium, iron, potassium, titanium, and magnesium.[13,14] In this way, it is well documented that the origin of life proceeded from minerals and clayish sediments. Hence, in the Precambrian era, the first organism has been suggested to have been formed by a mineral and an organic superstructure,[15] where the mineral part was constituted by Fe, Ni, S, H_2O, CO, and OH, whereas the organic superstructure was composed of CO, CO_2, COS, NH_3, H_2S, N_2, H_2, and HCN.[15] When analyzing the chemical composition proposed for the pioneer organism, one of the arising questions is: What is the explanation for the chemical composition of the first organism to be formed by iron (Fe) and not calcium (Ca)?

Received: September 29, 2021
Accepted: December 1, 2021
Published: December 15, 2021

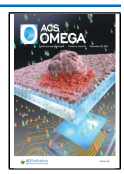

https://doi.org/10.1021/acsomega.1c05415
ACS Omega 2021, 6, 35629−35640

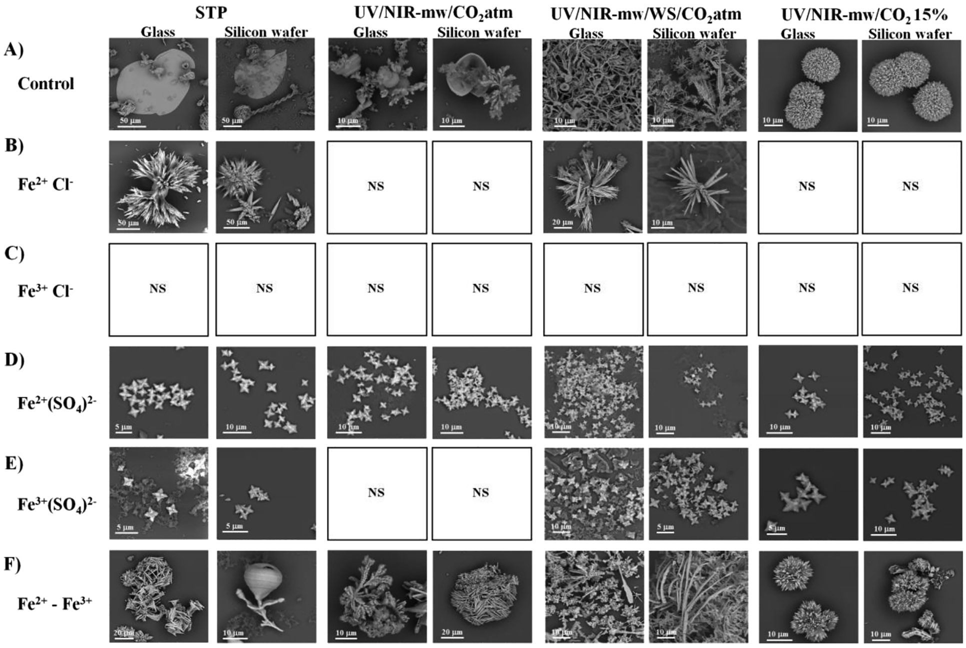

Figure 1. Morphologies obtained of the barium biomorphs synthetized under the following atmospheric conditions and the mixture of different ion composition: (A) control, (B) Fe^{2+}/Cl^{-}, (C) Fe^{3+}/Cl^{-}, (D) $Fe^{2+}/(SO_4)^{2-}$, (E) $Fe^{3+}/(SO_4)^{2-}$, and (F) Fe^{2+}/Fe^{3+}. Standard conditions (STP); UV/NIR-mw/CO_2atm; UV/NIR-mw/WS/CO_2atm; 15% UV/NIR-mw/CO_2. UV, ultraviolet light; NIR-mw, nonionizing microwave radiation; WS, water steam; CO_2atm, CO_2 from the environment; 15% CO_2, 15% CO_2 stream.

One explanation is that the oxidation of Fe during meteorization and diagenesis requires a lower exchange of redox equivalents with respect to the biological mechanisms mediated by Ca and S.[16] The second explanation is that it is possible that in the atmospheric conditions of the Precambrian era, the iron oxides contained in the sediments were formed as rocks, which favored that the first organism is formed in this type of rocks.[17,18] The third explanation is based on the Precambrian lutites formed by pyrite crystals (FeS_2); this information indicates that Fe^{2+} and sulfide ions were abundant in the seas of that era, which gave rise to the formation of lutites. Interestingly, as a step before the formation of pyrite crystals, the sulfide iron had been produced by the first sulfate-reducing bacteria. This datum is possibly the most direct evidence that iron was the main ion in the pioneer organism that allowed it to perform the first biological reactions. Therefore, iron is one of the chemical elements that has played a pivotal role in the origin and evolution of the different forms of life. The iron existing in the Precambrian, in a reducing atmosphere and being part of the first organism, became pyrite (FeS_2) with O_2-producing hematite (Fe_2O_3) and gypsum ($CaSO_4.2H_2O$) once the environment changed to an oxidizing atmosphere. Hematite (Fe^{3+}) played a relevant role in the early stage of the oxidizing atmosphere because it precipitated from the upper part of oceans due to its lower solubility compared with Fe^{2+}.[17] Although it has been proposed that iron was part of the pioneer organism, it is fundamental to know the structure adopted by that first cell in the presence of iron in the atmospheric conditions prevailing in the Precambrian era. To answer this and other questions, it is indispensable to have a model that will allow extrapolating the first chemical structures of the pioneer organism formed in the Precambrian. In this context, for several decades, in vitro structures chemically formed by silica-carbonates have been synthetized, called biomorphs, because they could emulate living organisms and might resemble primitive organisms.[19−26] Because biomorphs form structures with characteristic morphologies, they could resemble the microfossils found in the cherts of the Precambrian.[20] Their resemblance to the Precambrian microfossils is so evident that a detailed research using strict comparisons of these biomorphs with archaic microfossils could indicate that life did not generate in this geological era but, rather, that it is more recent. Actually, what has been dated are silica biomorphs that formed according to the chemical and physical conditions prevailing in that geological era, and their inclusion in sedimentary rocks is nothing else than a simple common biomineralization process.[27] Experimentally, it has been demonstrated that minerals, including clays (clays are very abundant orthosilicates in many parts of the Earth, planets, and satellites in space and could have played an important role in the chemical stereoselectivity of the biological macromolecules that participated in the chemical origin of life), participated in the concentration, alignment, and polymerization of the first biomolecules, giving rise to the first organism in the Precambrian era.[28,29] Another characteristic of these compounds is that the adopted morphology could go from emulating organisms to a spherical morphology or no morphology at all.[24,25] Due to these unique characteristics, the silica-carbonate compounds are a good study model to evaluate the different morphologies that could have been adopted by the first organisms in the primitive era of the Earth. Aiming to understand how iron participated in the formation of the first chemical structures of the primitive organisms, we assessed how iron contributes to the morphology and chemical−crystalline structure during the synthesis of these biomorphs in different conditions prevailing in the primitive atmosphere.

https://doi.org/10.1021/acsomega.1c05415
ACS Omega 2021, 6, 35629−35640

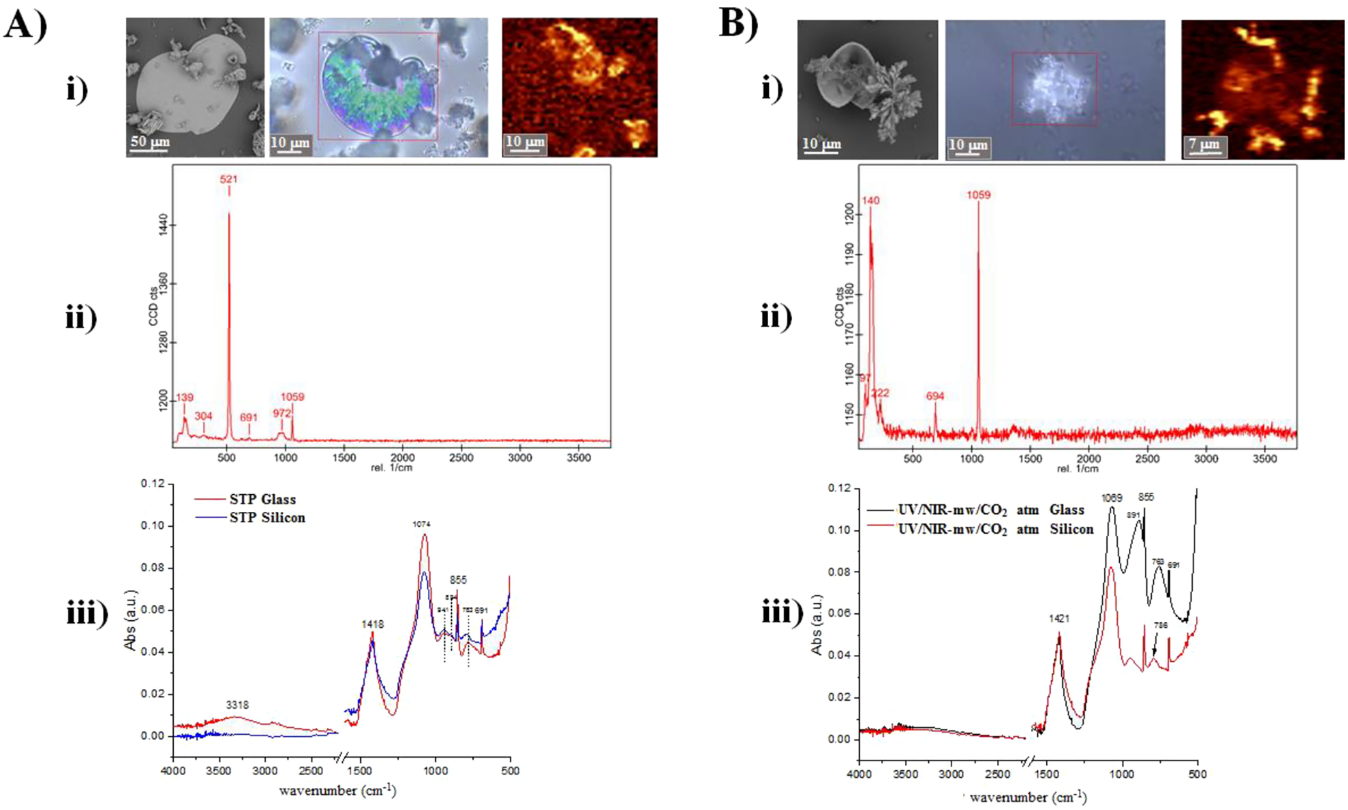

Figure 2. Identification of the crystalline base of the $BaCO_3$ biomorphs through Raman spectroscopy and FTIR. (A) Control sample. (B) Sample synthetized with UV light. (i) SEM, optical, and confocal images. (ii) Raman spectra. (iii) FTIR spectra. The $BaCO_3$ biomorphs show a witherite crystalline structure.

2. RESULTS AND DISCUSSION

2.1. Water Steam Together with UV Light Are the Atmospheric Conditions that Allow Obtaining Biomorphs Emulating Complex Life Form Groupings. To determine the influence of iron on the morphology of the biomorph during its synthesis and to know whether the crystalline structure is modified in the presence of iron in either oxidation number (Fe^{2+}, Fe^{3+}) with different anions (Cl^-, SO_4^{2-}), as well as in both oxidation states (FeO, Fe_2O_3), we evaluated the formation of barium silica-carbonates in the presence of the five compounds, $FeCl_2 \cdot 4H_2O$, $FeCl_3 \cdot 6H_2O$, $FeSO_4 \cdot 7H_2O$, $Fe_2(SO_4)_3 \cdot H_2O$, and $FeO \cdot Fe_2O_3$, in four different atmospheric conditions. It was decided to perform the synthesis of biomorphs on glass or on silicon wafers to assess whether the composition of the support material affects the morphology of the formed biomorph because, chemically, glass is mainly formed by SiO_2 (silica), B_2O_3, and P_2O_5 oxides, whereas the silicon wafer is formed by crystalline silicon. To emulate the Precambrian conditions where these conditions have been reported in comparison to the current atmosphere,[30,31] experiments were performed under different conditions, including UV light, nonionizing microwave radiation (NIR-mw), water steam (WS), and CO_2, obtaining a total of 48 different conditions (Figure 1). Once synthetized, biomorphs were observed through SEM. As seen in Figure 1, the control silica-carbonates obtained in standard conditions of temperature, pressure, and CO_2 (STP) depict a morphology of leaves and helices on both glass and silicon wafers (Figure 1A), which correspond to characteristic morphologies of the biomorphs previously reported.[19−26]

The combination exposed to UV and NIR-mw revealed a morphology emulating different shells with leaves and stems on both support materials (Figure 1A). We chose to work with two types of nonionizing radiations, short waves of UV light, and long waves of microwaves (mw),[32] because solar radiation emits both types of radiations and it is the energy source needed for the existence of life on Earth; the origin of the first biomolecule (RNA), the emergence of the primitive organism, the evolution and perpetuation of life, and ensuring the continuity of the different species are all tied to sunlight. The sun emits gamma, X, and UV (visible and infrared) rays of which we receive, on the terrestrial surface, part of the UV light, visible, and near-infrared. UV light is divided in three types: UVC (100−280 nm), UVB (280−315 nm), and UVA (315−400 nm); however, the ozone layer allows only a minimal amount of UVA and UVB to reach the Earth.[33] Both UVA and UVB directly affect chemical molecules because they can generate free radicals, making the molecules very reactive and altering the global chemical reaction. Notwithstanding, the amount of midday radiation received by the terrestrial atmosphere is of 95% UVA.[34,35] The change in morphology of the sample exposed to UV/NIR-mw, compared to the nonexposed sample (Figure 1A), could be because the UV light generated photoionization of the molecules contained in the reaction mixture, changing the structural arrangement of the biomorphs. This result agrees with other works that have shown that UV light modifies the structure of molecules. Oparin was one of the pioneering researchers suggesting that the UV radiation could have favored the chemical reaction to generate the first molecules.[36,37] Urey and Miller showed that, starting with a primitive mixture in conditions emulating the

https://doi.org/10.1021/acsomega.1c05415
ACS Omega 2021, 6, 35629−35640

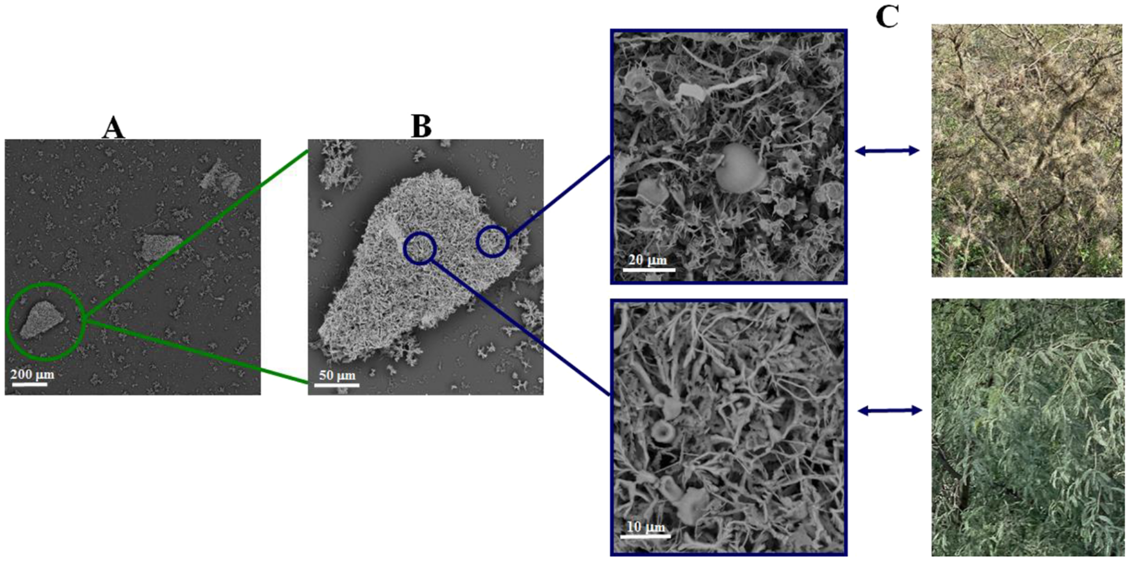

Figure 3. Micrographs of silica-$BaCO_3$ biomorphs synthetized in the presence of UV/NIR-mw/WS. (A) Clusters of the silica-$BaCO_3$ crystals observed at a magnification of 100×. (B) Magnification of clusters at 500×. (C) Magnification of a part of the clusters at 3000×, revealing clusters that emulate foliage due to the dense network of leaves, stems, and flowers that were synthetized. The double-direction arrows show the similitude in the morphology of the silica−barium carbonate biomorphs obtained by synthesis with the foliage of nature.

atmosphere of the Precambrian era, amino acids and organic chemical compounds can be obtained.[38,39] In a more recent work, it was shown that the photolysis of 5-substituted hydantoin by UV light leads to obtain amino acids and imidazolidinedione.[40] In more complex organisms, like plants, these have adapted to high radiations of this UVB light; thus, their branches, stems, and internodes are shorter compared to plants not exposed to high radiation.[41−44] The diminution in the size of their organs is due to UVB affecting different biomolecules and, hence, modifying the metabolic processes. These works reveal that UV light has exerted a fundamental role not only in the chemical origin of life but also in the origin and modification of the different morphologies adopted by organisms.

To analyze whether a change in the chemical and crystalline structure occurred in the barium biomorphs synthetized with or without UV/NIR-mw, Raman and FTIR techniques were used. These methods were chosen because Raman is a high-resolution method that provides, in a few seconds, chemical and structural information of any organic and inorganic compound, allowing for the identification of the polymorphs.[45] FTIR is a powerful technique that provides information on the structure and molecular concentration of each compound.[46,47] Bands of 139, 304, 521, 691, 972, and 1059 cm^{-1} were identified in the Raman spectra corresponding to the control samples synthetized on glass or on the silicon wafer (Figure 2Aii).

These vibrations correspond to $BaCO_3$(I) in its aragonite-type crystalline structure, called witherite, which belongs to the orthorhombic space group.[48,49] Regarding the samples of barium biomorphs synthetized under UV/NIR-mw, the characteristic bands reported for the silica-carbonate biomorph were found in its witherite crystalline structure just as found in the control sample (Figure 2Bii). When analyzing the microstructure of the barium silica-carbonate crystals with FTIR, the spectra of the samples in STP conditions showed peaks at 691, 783, 855, 1074, 1418, and 3318 cm^{-1} (Figure 2Aiii). The biomorphs obtained with exposure to UV/NIR-mw showed peaks at 691, 786, 855, 1069, and 1421 cm^{-1} (Figure 2Biii). In both conditions, the peaks correspond to those reported for $BaCO_3$ crystals.[50] It is well documented that the peaks at 855, 783, and 691 cm^{-1} are found in the in-plane and out-of-plane bending of CO_3^{2-}.[50] The IR bands at 1418 cm^{-1} correspond to the asymmetric stretching mode of the C−O bond, and the peak at 1074 cm^{-1} corresponds to the symmetric C−O stretching vibration.[50] These data reveal that the chemical composition and the chemical structure are not modified by the presence of UV light (Figure 2) in contrast to the morphology, which is modified as previously described (Figure 1A).

Another biomorph synthesis condition to be evaluated was the morphology and crystalline structure in the presence of water steam. The aim of studying biomorph synthesis in two or more conditions that predominated in the Precambrian era was to know if there is a predominating atmospheric factor. In this third condition, biomorphs were obtained under UV/NIR-mw and water steam (UV/NIR-mw/WS) conditions. WS was chosen because there is controversy in this aspect; some authors have interpreted that the silicon isotopes found in the cherts imply seawater temperatures from 60 to 80 °C,[51] whereas other research groups have argued that the hyper-thermophilic microorganisms that dwell at temperatures of 110 °C, as well as those organisms that inhabit the Earth at other temperatures, do not indicate an origin of life at these temperatures.[52,53] In addition, some authors consider that in the Precambrian era, the WS favored the formation of primeval oceans, in which the start of life is postulated to have occurred in volcanic vents at least 3.2 Ga, where the first chemical reactions were generated.[54] Barium biomorphs obtained in UV/NIR-mw/WS condition in glass and silicon wafers presented a morphology of leaves, stems, and flowers (Figure 1A). Interestingly, in these conditions, the formation of leaves, stems, and flowers had an unusual growth not reported previously because clusters were observed (Figure 3A). Magnification of the clusters at 500× (Figure 3B) revealed a complex network. A higher magnification at 3000× revealed

https://doi.org/10.1021/acsomega.1c05415
ACS Omega 2021, 6, 35629−35640

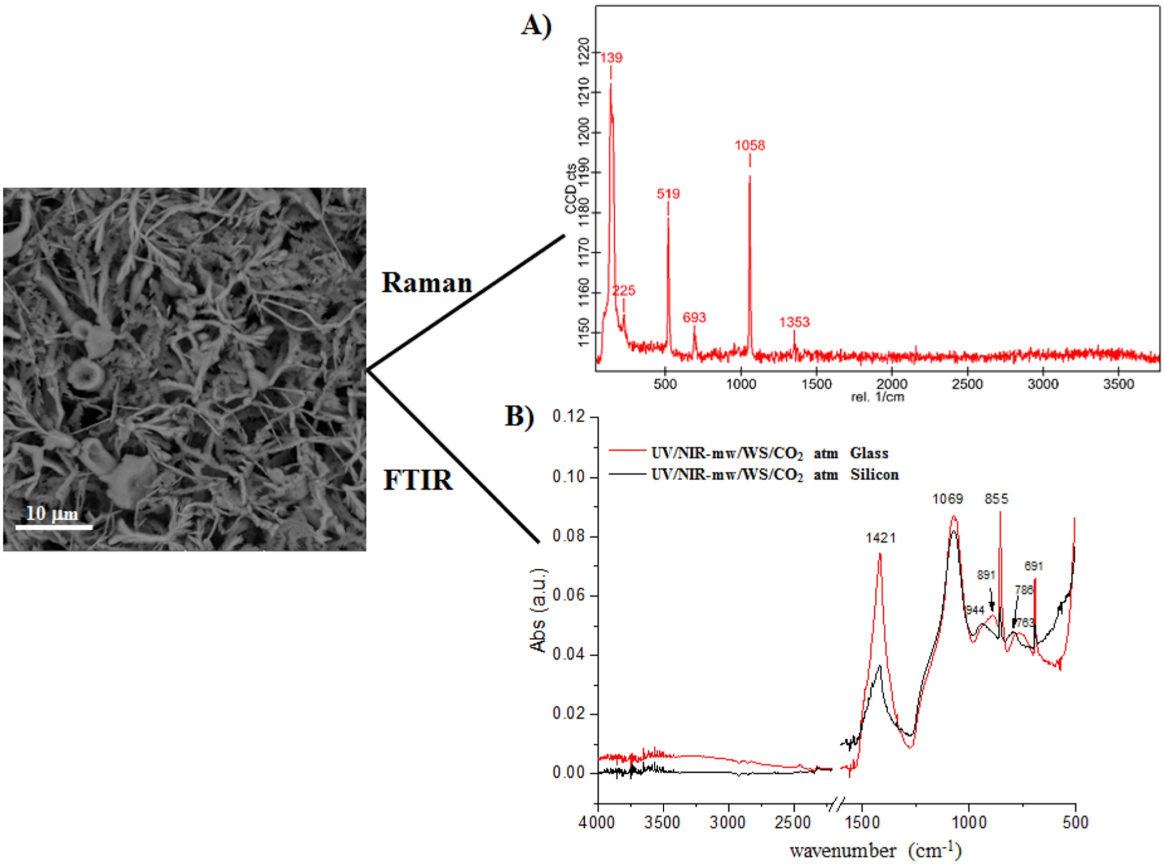

Figure 4. Analysis of biomorphs synthetized under UV/NIR-mw/WS/CO_2 atmosphere. Identification of the crystalline phase of the biomorphs by (A) Raman and (B) FTIR spectroscopy.

that these clusters emulate foliage due to the dense network of leaves, stems, and flowers that were synthetized (Figure 3C).

Other works have shown that the morphology of the biomorphs synthetized at high temperature varies—for example, at 45 °C, biomorphs emulate flowers and twisted ribbons; at 60 °C, leaves and filamentous clusters have been observed; and at 70 °C, star-shaped clusters have been observed.[55] However, the crystalline clusters that we obtained in the presence of UV/NIR-mw/WS have not been observed (Figure 3). A possible explanation for the dense network that emulates the foliage in nature is that the water steam favored the $BaCO_3$ chemical groups to grow in both length and width when the crystals became intertwined, as shown by the growth of the $BaCO_3$ crystals obtained under a controlled hydrothermal growth.

As a whole, these results show that by the presence of these two atmospheric conditions in the Precambrian era (UV and WS), it was chemically possible for more complex structures to be formed from few chemical elements. This could evidence that organisms like plants adopted this morphology since the primitive era, and has been modified along the years. In this way, some chemical elements have been incorporated until the plants acquired the functions and chemical composition as we know them nowadays. This hypothesis is based on reports through protein sequencing analyses that before plants, 1000 Ma ago, a bacterial flora of cyanobacteria existed, which are algae that emulated the morphology of plants and took volcanic chemical elements in the water as source of food and energy.[56] Later on, terrestrial plants appeared at 700 Ma together with green algae and the first fungi, contributing to the change from a reducing atmosphere to an oxidizing one, allowing in this way the origin of multicellular organisms in the Precambrian era.[57] Our data and the reports of other research teams foster the hypothesis that the first bacterial cells had their origin at hydrothermal vents because, as observed, the WS favored importantly the formation of barium biomorphs in dense clusters that emulate the morphology of foliage (Figure 3). The Raman analysis of the barium biomorphs synthetized in these two atmospheric conditions, either on glass or silicon wafer, showed bands at 139, 225, 519, 693, 1058, and 1353 cm^{-1} (Figure 4A). These bands correspond to $BaCO_3$ in its witherite polymorph. Additionally, results of FTIR showed peaks at 691, 763, 786, 855, 891, 944, 1069, and 1421 cm^{-1} (Figure 4B). In both conditions, the peaks correspond to those reported for $BaCO_3$ crystals.[50] These results are relevant because they show that the crystalline structure of the $BaCO_3$ biomorph is conserved in either atmospheric condition; however, the morphology and growth of the crystals are changed depending on the atmospheric condition to which they are subjected during the synthesis.

This is perhaps the most plausible explanation as to why most organisms from unicellular to multicellular are formed by the same chemical elements but with different morphologies as a result of the atmospheric conditions in Earth.

The fourth condition considered was to assess the influence of carbon dioxide (CO_2) on the morphology and crystalline structure of the barium biomorphs. CO_2 has been reported by some authors as one of the dominant gases in the Precambrian era,[58,59] whereas other authors have indicated that CO_2 cannot remain in the atmosphere for a long time.[60−62] It is converted

https://doi.org/10.1021/acsomega.1c05415
ACS Omega 2021, 6, 35629−35640

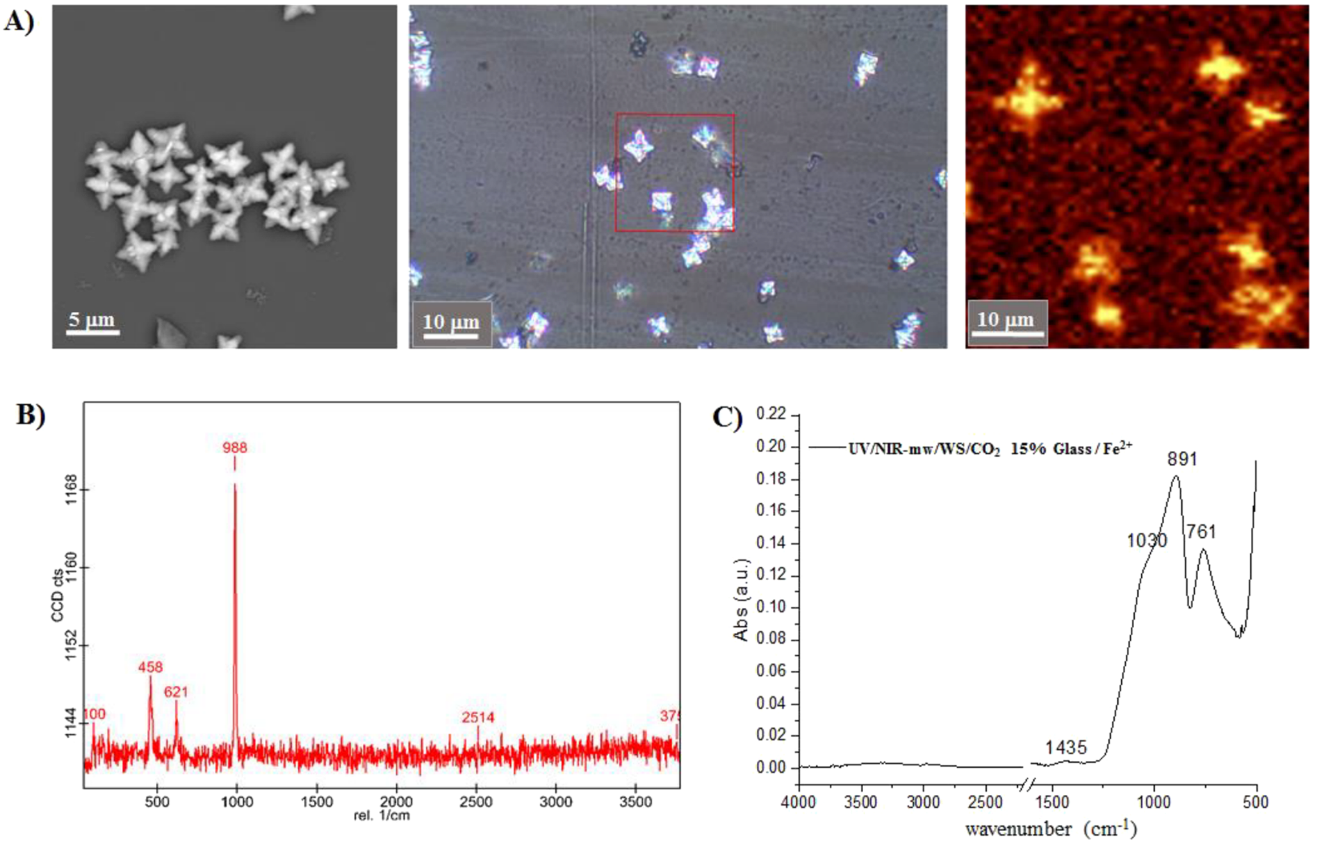

Figure 5. Representative image of the biomorphs obtained in the presence of Fe^{2+} in the four atmospheric conditions analyzed in this study: STP, UV/NIR-mw/CO_2atm, UV/NIR-mw/WS/CO_2atm, or UV/NIR-mw/CO_2 15%. (A) SEM, optical, and confocal images. (B, C) Identification of the crystalline phase of the biomorphs through (B) Raman and (C) FTIR spectroscopy.

through a chemical reaction that yields calcium carbonate ($CaCO_3$) and silicon oxide (SiO_2); this process enables the dissolution of $CaCO_3$ from rocks. Through this set of reactions, the CO_2 in the atmosphere and soil, during the early era of the Earth, diminished its concentration.[63] In addition, it has been reported that light, together with CO_2, has played a fundamental role in the chemical origin of life as demonstrated by the early experiments of Oparin, Urey, and Miller in which they emulated the conditions of the Precambrian environment, obtaining organic compounds.[36−39] From those experiments up to now, it has been demonstrated that UV light produces photodissociation of CO_2-yielding O_2.[64] This is evidence revealing that the high energy of the UV light was able to produce O_2 in the reducing atmosphere prevailing in the Precambrian era, which would favor the hypothesis that the CO_2 concentration in the atmosphere could not have been high because, on one side, O_2 would be formed with the UV light and, on the other side, $CaCO_3$ and silicon oxide (SiO_2) would be formed as postulated by diverse research teams.[36−39,63] To assess the effect of a high CO_2 concentration in the presence of UV light on the morphology of barium biomorphs, we synthetized biomorphs in the presence of UV light and under a current of 15% CO_2 (UV/NIR-mw/CO_2 15%) (Figure 1A). As shown in Figure 1A, the barium biomorphs obtained in these atmospheric conditions presented a morphology of spheres. The spherulitic morphology in biomorphs has been found in other synthesis conditions.[24,25] Although this morphology could be reminiscient of the morphology of the first bacteria, at a high CO_2 concentration, the morphologies that resemble life forms would not be possible. This event suggests that the presence of O_2 in the first photosynthetic bacteria and in the photolysis of CO_2 modified the environmental atmosphere and favored the synthesis of other morphologies that, in conjunction, gave rise to the diverse chemical structures constituting the terrestrial organisms.

The Raman spectrum of the spheres obtained in the presence of UV/NIR-mw/CO_2 15% showed bands at 96, 139, 155, 225, 692, and 1059 cm^{-1} (Figure S1A). These bands correspond to $BaCO_3$ in its witherite polymorph. FTIR results showed peaks at 692, 777, 855, 892, 1059, 1417, and 2452 cm^{-1} (Figure S1B). In both conditions, peaks correspond to those reported for $BaCO_3$ crystals.[50] As observed with the different environmental factors that emulate the atmosphere existing in the Precambrian era, the origin of the diverse morphologies that reminisce terrestrial organisms (leaves, flowers, stems, helices, and ribbons, among others) were probably formed mostly at lower CO_2 concentrations, with water steam being probably one of the determining atmospheric factors for the obtainment of morphologies emulating different forms of life. These data agree with the hypothesis of some research groups, suggesting that CO_2 cannot remain in the atmosphere for a long time.[60−62]

2.2. Versatility of the Oxidation Potential of Fe^{2+}/Fe^{3+} Enables the Formation of Diverse Morphologies of Complex Chemical Composition. It has been suggested that iron has been part of the chemical composition of the pioneer organism.[15] However, one of the questions that still remain without any answer is: Why is it proposed that this first organism was formed by iron (Fe) and not by calcium (Ca) or

https://doi.org/10.1021/acsomega.1c05415
ACS Omega 2021, 6, 35629−35640

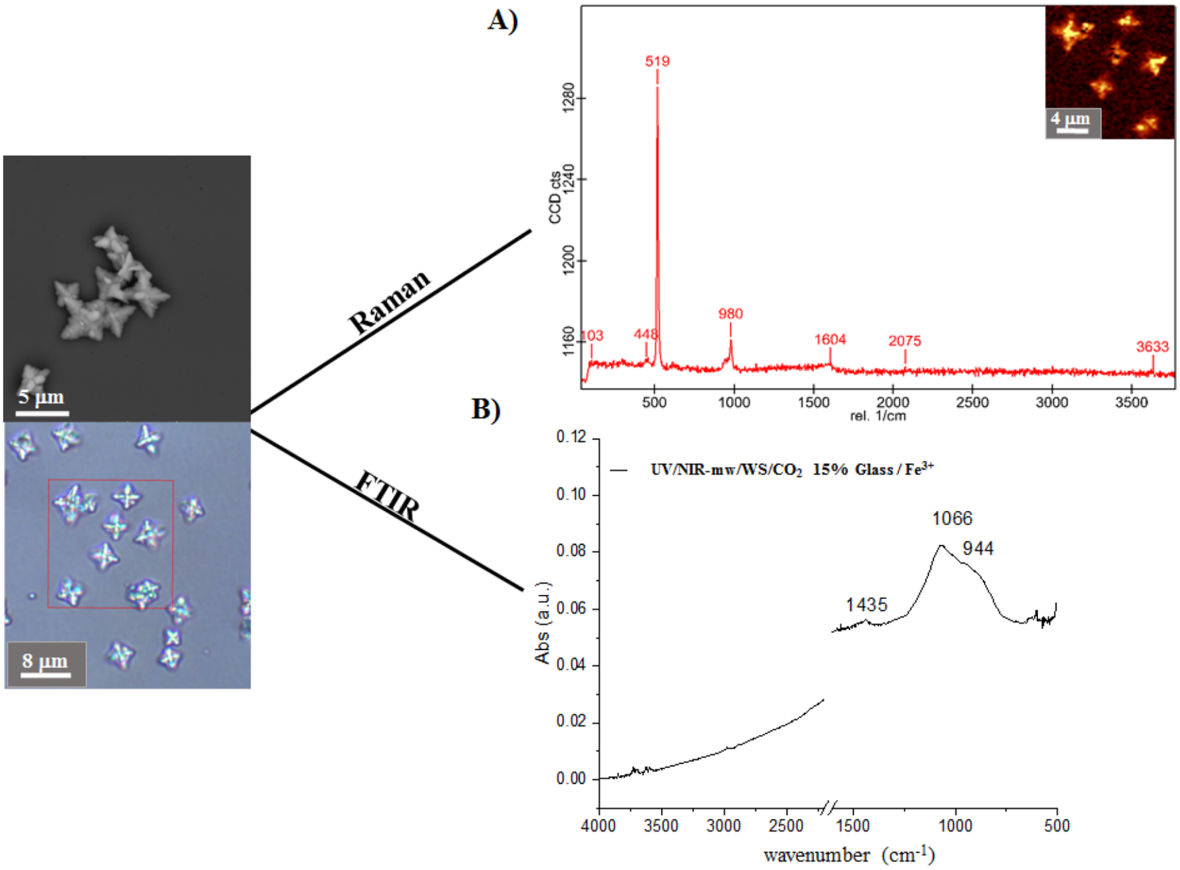

Figure 6. Representative image of the biomorphs obtained in the presence of Fe^{3+} (SEM, optical, and confocal images), in the four analyzed atmospheric conditions: STP, UV/NIR-mw/CO_2atm, UV/NIR-mw/WS/CO_2 atm, or UV/NIR-mw/CO_2 15%. Identification of the crystalline phase of biomorphs through (A) Raman and (B) FTIR spectroscopy.

another chemical element? In order to elucidate this question, we performed the synthesis of biomorphs in the previously described atmospheric conditions (Figure 1A) in the presence of $Fe^{2+}2Cl^{-}$ or $Fe^{3+}3Cl^{-}$. We chose to work with both iron oxidation states to know whether the morphology of biomorphs changes or is conserved depending on the oxidation number of iron. The latter is based on the report that in the iron cycle, in nature, most of the reduced iron is part of sedimentary rocks, whereas ferrous Fe is oxidized by weathering.[16] After performing the synthesis of biomorphs in the four atmospheric conditions (STP, UV/NIR-mw/CO_2atm, UV/NIR-mw/WS/CO_2atm, or UV/NIR-mw/CO_2 15%) in the presence of Fe^{2+}or Fe^{3+} and observing the samples through SEM to know the formed morphology, surprisingly, we found that the synthesis of biomorphs had not been accomplished (Figure 1B,C). Notwithstanding, with Fe^{2+} in the STP and UV/NIR-mw/WS/CO_2 atm conditions, some biomorphs in the form of spherulite-like structures were scarcely identified (Figure 1B). Identification of the chemical composition and the crystalline structure of these biomorphs through both Raman and FTIR in both conditions revealed that they correspond to $BaCO_3$ in the witherite polymorph (data not shown). Based on these results, the next question arose: Does iron inhibit the synthesis of biomorphs, or is the chloride ion responsible for the unfavorable chemical reaction and, hence, the synthesis of biomorphs is not accomplished? To answer these two questions, we decided to use $FeSO_4$ and $Fe_2(SO_4)_3$, where the anion is the sulfate ion SO_4^{2-}. After performing the synthesis, when visualizing the samples through SEM, we found that in the four tested atmospheric conditions, as well as in the presence of Fe^{2+} or Fe^{3+}, the morphology of the biomorphs was in the shape of stars (Figure 1D,E), except for the UV/NIR-mw/CO_2atm with Fe^{3+}condition where no synthesis of biomorphs was accomplished (Figure 1E). This result reveals that Fe^{3+} in the presence of UV light and CO_2 at low concentration is not a favorable condition for the synthesis of biomorphs. The latter is possible because iron, being in an oxidized state and in these atmospheric conditions, is insoluble and behaves as a weak acid as observed in other conditions,[65] indicating that water steam or a higher concentration of CO_2 is required for the Fe^{3+} to be available for the formation of biomorphs. Once the morphology of biomorphs in the presence of Fe^{2+} or Fe^{3+} had been observed (Figure 5A), Raman and FTIR were applied to know the chemical composition and crystalline structure. Samples in the presence of Fe^{2+}, in the Raman analysis, showed peaks at 100, 458, 621, 988, and 2514 cm^{-1} (Figure 5B). These peaks correspond to a mixture of $BaCO_3$, $FeCO_3$, and FeO according to the Raman spectra reported for these compounds.[48,49,66−69] The FTIR spectrum showed bands at 761, 891, 1030, and 1435 cm^{-1}, which corroborated that the stars' morphology obtained in all conditions in the presence of Fe^{2+} corresponds to $BaCO_3$, $FeCO_3$, and FeO (Figure 5C).[50,70]

For the biomorphs synthetized in the presence of Fe^{3+}, the Raman spectrum identified peaks at 103, 448, 519, 980, 1604, and 2075 cm^{-1} (Figure 6A). These bands correspond to $BaCO_3$, Fe_2O_3, and $Fe_2(CO_3)_3$.[48,49,66−69] The FTIR spectrum

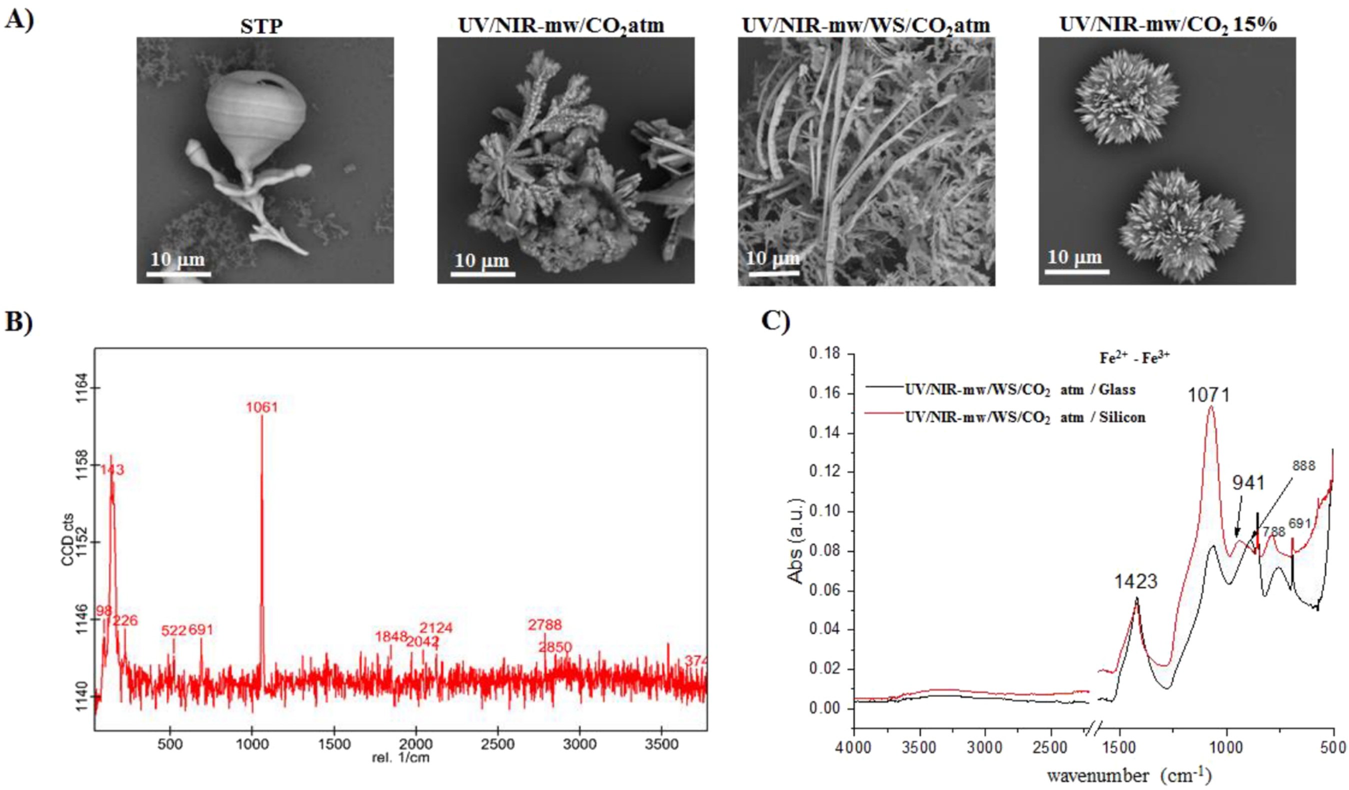

Figure 7. Representative images of the biomorphs obtained in the presence of the Fe^{2+}/Fe^{3+}mixture with the four analyzed atmospheric conditions: STP, UV/NIR-mw/CO_2atm, UV/NIR-mw/WS/CO_2atm or UV/NIR-mw/CO_2 15%. (A) Identification of the crystalline phase of biomorphs by (B) Raman and (C) FTIR spectroscopy.

identified the characteristic peaks revealed by Raman spectroscopy (Figure 6B).[50,70]

The star morphology obtained with iron in either oxidation state led us to question whether placing both ions (Fe^{2+}, Fe^{3+}) in the reaction mixture would conserve the same star morphology or it would be susceptible to be changed. To respond to this query, we included the Fe^{2+} and Fe^{3+} ions in the reaction mixture at an equimolar concentration, and this mixture was exposed to each one of the four assessed atmospheric conditions (STP, UV/NIR-mw/CO_2atm, UV/NIR-mw/WS/CO_2atm, or UV/NIR-mw/CO_2 15%). Biomorphs synthetized in standard atmospheric conditions (STP) presented a morphology of flowers and arrangements (Figure 1F), whereas biomorphs obtained under UV/NIR-mw/CO_2atm conditions showed morphologies of leaves and spheres formed by leaves (Figure 1F). Biomorphs produced with UV/NIR-mw/WS/CO_2atm presented a morphology of stems and leaves (Figure 1F), with the same density as that observed without Fe (Figure 1A). Finally, the morphology of the biomorph treated with UV/NIR-mw/CO_2 15% was of spheres (Figure 1F). Once we found that iron must count upon the two oxidation numbers to enable the formation of different morphologies (Figure 7A), we analyzed the chemical composition of the biomorphs to determine whether barium had been displaced by iron or it was still conserved in the structure. Once the morphology of the biomorphs in the presence of both iron cations had been observed, we proceeded to know their chemical composition. Raman spectroscopy revealed peaks at 98, 143, 226, 522, 691, 1061, 1358, 1495, 1788, 1848, 2042, 2124, and 2788 cm^{-1} (Figure 7B).

With these peaks, we identified that the structures were formed by $BaCO_3$, δ-FeOOH, $Fe^{3+}O(OH)$, α-Fe_2OH, $FeCO_3$, and $Fe_2(CO_3)_3$.[48,49,66−69] The FTIR spectrum identified the peaks confirming the compounds by Raman (Figure 7C).[50,70] In contrast to the morphologies obtained in the control samples (Figure 1A), morphologies produced with Fe^{2+}/Fe^{3+} are more chemically complex (Figures 5−7). The versatility depicted by Fe with respect to another chemical element, like barium, is extraordinary because, although the obtained morphologies emulate organisms with barium (Figure 1A), they possess only one single chemical element (Figures 1−4 and Figure S1); with Fe^{2+}/Fe^{3+}, morphologies of organisms are also obtained but with a complex chemical composition (Figures 5−7).

As a whole, these results are of special interest because, as shown, when iron is found with the chloride ion (Cl^-), the chemical reaction cannot take place (Figure 1B,C), whereas in the presence of another anion like sulfate (SO_4^{2-}), the chemical reaction is favored toward a single morphology. This morphology that emulates a starfish or star-shaped bacteria like those of the *Stella* genus[71] could be one of the first morphologies possibly adopted by the pioneering organisms in the Precambrian era, since its chemical composition is reduced to iron carbonate and iron oxide (Figures 5 and 6). For bacteria of the *Stella* genus, it is known that their habitat is fresh and residual waters and they live at low nutrient concentrations in the soil.[71] This information, in conjunction with our results, could be indicative that, indeed, as postulated by Wächtershäuser in 2006, the first organism must have been formed by iron.[15] Hence, the next question is: how was it possible that from the primitive organism, other morphologies arose and with them, other organisms? As shown, when the

https://doi.org/10.1021/acsomega.1c05415
ACS Omega 2021, 6, 35629−35640

two iron ions (Fe^{2+}, Fe^{3+}) are present, morphologies that emulate higher organisms, like plants, are obtained (Figures 1F and 7A). The fact that iron can be oxidized or reduced, going from an oxidized state to a reduced one and vice versa in the environment as has occurred since the Precambrian era[16,72] favored the emergence of other morphologies and with them, other organisms with a higher number of chemical compounds from the primitive organisms (Figure 7B,C). This hypothesis agrees with the current knowledge on iron in organisms. Thus, from the biological point of view, the potential of the Fe^{2+}/Fe^{3+} oxidation/reduction makes iron extremely versatile when it is incorporated as an electron carrier.[73] In humans, iron exerts vital functions as it is part of numerous enzymes[74] and proteins, like transferrins, lactoferrins, and ferritins. Ferritins are found in animals, vegetables, and microorganisms.[75−77] Hemoglobin is another protein where Fe plays a fundamental role, as it allows capturing oxygen molecules keeping the human body oxygenated. Also, Fe is essential to produce energy and protect cells against free radicals and bacteria-producing free radicals as part of the immune response. It has also been described that in certain physiological processes, like those occurring in enterocytes of the gastric lumen and the proximal duodenum, Fe is oxidized or reduced, respectively.[78,79] In microorganisms, Fe is extremely necessary for their vital functions; they have developed siderophores, which are molecules secreted by them in deficient conditions to sequester iron from their surroundings.[80,81] Plants also need Fe for their functions; it avoids chlorosis, participates in their oxygenation or respiration, and helps form chlorophyll. Plants benefit mainly from the Fe available in the soil through microbial siderophores.[82−84] As explained, iron is essential for the vital functions of any terrestrial organism from bacteria to higher organisms; this is probably because since the formation of the first cell in the Precambrian era, it played a preponderant role in the origin, maintenance, and evolution of life.

3. CONCLUSIONS

The chemical origin of life is the conjunction of multifactorial events, both atmospheric and chemical, that allowed for the synthesis of the first biomolecules, which jointly favored the origin of the pioneer organism. This pioneer organism has been proposed to be formed by the chemical compounds most abundant in the Precambrian era, like iron (found in minerals like hematite). Our data suggest that apparently, iron, from the first organism until nowadays, has played a fundamental role in the evolution of terrestrial living beings because iron fosters the formation of several morphologies with a more complex chemical composition. The latter could have favored the evolution of the pioneer organism to more complex life forms. To the best of our knowledge, this is the first work where, from a model like the biomorphs, the participation of iron is evaluated in the morphology and chemical composition that the pioneering organism might have had. This work aims at contributing to the long path that still has to be discovered regarding the chemical origin of life.

4. EXPERIMENTAL SECTION

4.1. Synthesis of Biomorphs with Iron under Different Atmospheric Conditions.

The biomorphs were obtained by the gas diffusion method.[85] Synthesis was performed on glass or silicon squares of 1 mm thickness. Synthesis of biomorphs was performed with both substrates to assess whether the morphology changes or is retained on an ordered substrate (as is the case of the silicon disk that is crystalline) with respect to another that is not ordered (like glass, where the atoms are randomly arranged). The used glass or silicon square had a size of 5 mm in length and 5 mm in width. The glass or silicon square was placed in a crystallization cell, where 1000 ppm of sodium metasilicate and 20 mM barium chloride ($BaCl_2$) were added; this mixture was aliquoted in equal volumes, and each aliquot was supplemented with one of the following compounds: $FeCl_2.4H_2O$, $FeCl_3.6H_2O$, $FeSO_4.7H_2O$, $Fe_2(SO_4)_3.H_2O$, mixed oxide ($FeO.Fe_2O_3$ or Fe_3O_4), at a concentration of 20 mM. The pH of the mixture was adjusted to 11.0 with sodium hydroxide. All reagents were from Sigma-Aldrich (St. Louis, MO, USA). Biomorphs were synthetized in the following conditions: (1) standard conditions of temperature, pressure, and CO_2 (STP); (2) UV radiation at 325 nm (UV) during 10 min, followed by nonionizing microwave radiation (NIR-mw) during 5 min; (3) UV/10 min, followed by NIR-mw/5 min, water steam (WS) during 15 min, under an atmospheric CO_2 current; and (4) UV/10 min, followed by NIR-mw/5 min, WS/15 min, under a constant CO_2 current at 15 or 5% at 37 °C. In each of the four conditions, the synthesis of biomorphs was performed in 24 h. Experiments were made in triplicate.

4.2. Characterization of Biomorphs.

Biomorphs were observed through scanning electron microscopy (SEM) and analyzed through Raman microspectroscopy and Fourier transform infrared (FTIR) microspectroscopy.

4.2.1. Scanning Electron Microscopy. Biomorphs were observed by means of SEM microphotographs in a TESCAN microscope (Brno, Czech Republic) model VEGA3 SB with a secondary electron detector (SE) from 10 to 20 kV in high vacuum conditions (work distance of 10 mm).

4.2.2. Raman Microspectroscopy. Raman spectrum measurements were recorded with a WITec Alpha300 R (WITec GmbH, Ulm, Germany) using a 672 lines/mm grating and 532 nm laser light excitation originated from a Nd:YVO4 green laser. The incident laser beam with a power of 14.4 mW was focused by 20, 50, and 100× objectives (Zeiss, Germany) with 0.4, 0.75, and 0.9 NA, respectively. Punctual Raman spectra were obtained with 0.5 s of integration time and 10 accumulations, and the Raman map was obtained using 0.01 s of integration time. The data processing and analysis were performed with WITec Project Version 5.1 software.

4.2.3. Fourier Transform Infrared Spectroscopy (FTIR). Fourier transform infrared spectroscopy (FTIR) analysis was made in a Nicolet iS50R Thermo Scientific (Waltham, MA, USA) spectrometer equipped with an attenuated total reflectance (ATR) diamond crystal accessory (Smart-iTX). Spectra acquisitions were collected with 32 scans with 4 cm^{-1} of spectral resolution in the range of 525 to 3600 cm^{-1}. Additionally, the iron salts were used to form KBr pellets for FT-IR spectrum measurements on the same spectrophotometer in the transmittance mode. The data processing and analysis were performed with OriginPro version 2021 software.

■ ASSOCIATED CONTENT

Supporting Information

The Supporting Information is available free of charge at https://pubs.acs.org/doi/10.1021/acsomega.1c05415.

(Figure S1). Analysis of biomorphs synthetized under UV/NIR-mw/WS/CO_2 15%; identification of the crystalline phase of the biomorphs by (A) Raman and (B) FTIR spectroscopy (PDF)

AUTHOR INFORMATION

Corresponding Author

Mayra Cuéllar-Cruz − *Departamento de Biología, División de Ciencias Naturales y Exactas, Campus Guanajuato, Universidad de Guanajuato, C.P. 36050 Guanajuato, Guanajuato, México;* orcid.org/0000-0002-6616-7917; Email: mcuellar@ugto.mx

Author

Selene R. Islas − *Instituto de Ciencias Aplicadas y Tecnología, Universidad Nacional Autónoma de México, Ciudad de México 04510, México*

Complete contact information is available at: https://pubs.acs.org/10.1021/acsomega.1c05415

Notes

The authors declare no competing financial interest.

ACKNOWLEDGMENTS

This work was carried out with the financial support granted to M.C.-C. by project no. CF2019-39216 from the Consejo Nacional de Ciencia y Tecnología (CONACYT) and Proyecto Institucional UGTO-022/2021 from Universidad de Guanajuato, México. The authors acknowledge Ms. Ingrid Mascher for the English revision of this manuscript. The authors acknowledge LUCE-ICAT for characterization of the samples and Dayra Betzabé Barreto Hernández for valuable help.

REFERENCES

(1) Schopf, J. W.; Kvenvolden, K. A.; Barghoorn, E. S. Amino acids in Precambrian sediments: an assay. *Proc. Natl. Acad. Sci. U. S. A.* **1968**, *59*, 639−646.

(2) Schopf, J. W.; Barghoorn, E. S. Alga-like fossils from the early precambrian of South Africa. *Science* **1967**, *156*, 508−512.

(3) Schopf, J. W.; Barghoorn, E. S.; Maser, M. D.; Gordon, R. O. Electron microscopy of fossil bacteria two billion years old. *Science* **1965**, *149*, 1365−1367.

(4) Lopuchin, A. S. Structures of biogenic origin from Early Precambrian rocks of Euro-Asia. *Origins Life* **1975**, *6*, 45−57.

(5) Sergeev, V. N. Microfossils in cherts from the middle Riphean (Mesoproterozoic) avzyan formation, southern Ural Mountains, Russian Federation. *Precambrian Res.* **1994**, 231−254.

(6) Akiyama, M.; Shimoyama, A.; Ponnamperuma, C. Amino acids from the late Precambrian Thule group, Greenland. *Origins Life* **1982**, *12*, 215−227.

(7) Williams, K. M.; Smith, G. G. A critical evaluation of the application of amino acid racemization to geochronology and geothermometry. *Origins Life* **1977**, *8*, 91−144.

(8) Jacquemot, P.; Viennet, J. C.; Bernard, S.; Le Guillou, C.; Rigaud, B.; Delbes, L.; Georgelin, T.; Jaber, M. The degradation of organic compounds impacts the crystallization of clay minerals and vice versa. *Sci. Rep.* **2019**, *9*, 20251.

(9) Knoll, A. H. Paleobiological Perspectives on Early Microbial Evolution. *Cold Spring Harbor Perspect. Biol.* **2015**, *7*, a018093.

(10) Knoll, A. H.; Bergmann, K. D.; Strauss, J. V. Life: the first two billion years. *Philos. Trans. R. Soc., B.* **2016**, *371*, 20150493.

(11) McCarthy, E. D.; Van Hoeven, W.; Calvin, M. The synthesis of standards in the characterization of a C21 isoprenoid alkane isolated from Precambrian sediments. *Tetrahedron Lett.* **1967**, *8*, 4437−4442.

(12) Han, J.; Calvin, M. Occurrence of Fatty Acids and Aliphatic Hydrocarbons in a 3.4 Billion-year-old Sediment. *Nature* **1969**, *224*, 576−577.

(13) Clarke, F. W.; Washington, H. S. *The composition of the Earth's crust*; US Government Printing Office, 1924, *127*, 117.

(14) Taylor, S. R. Abundance of chemical elements in the continental crust: a new table. *Geochim. Cosmochim. Acta* **1964**, *28*, 1273−1285.

(15) Wächtershäuser, G. From volcanic origins of chemoautotrophic life to Bacteria, Archaea and Eukarya. *Philos. Trans. R. Soc., B* **2006**, *361*, 1787−1808.

(16) Kump, L. R.; Holland, H. D. Iron in Precambrian rocks: implications for the global oxygen budget of the ancient Earth. *Geochim. Cosmochim. Acta* **1992**, *56*, 3217−3223.

(17) Sand, K. K.; Jelavić, S. Mineral facilitated horizontal gene transfer: a new principle for evolution of life? *Front. Microbiol.* **2018**, *9*, 2217.

(18) Rosing, M. T.; Rose, N. M.; Bridgwater, D.; Thomsen, H. S. Earliest part of Earth's stratigraphic record: a reappraisal of the > 3.7 Ga Isua (Greenland) supracrustal sequence. *Geology* **1996**, *24*, 43−46.

(19) Zhang, G.; Morales, J.; García-Ruiz, J. M. Growth behaviour of silica/carbonate nanocrystalline composites of calcite and aragonite. *J. Mater. Chem. B* **2017**, *5*, 1658−1663.

(20) García-Ruiz, J. M.; Hyde, S. T.; Carnerup, A. M.; Christy, A. G.; Van Kranendonk, M. J.; Welham, N. J. Self-Assembled Silica-Carbons structures and detection of ancient microfossils. *Science* **2003**, *302*, 1194−1197.

(21) Opel, J.; Wimmer, F. P.; Kellermeier, M.; Cölfen, H. Functionalisation of silica-carbonate biomorphs. *Nanoscale Horiz.* **2016**, *1*, 144−149.

(22) Voinescu, A. E.; Kellermeier, M.; Bartel, B.; Carnerup, A. M.; Larsson, A. K.; Touraud, D.; Kunz, W.; Kienle, L.; Pfitzner, A.; Hyde, S. T. Inorganic Self-Organized silica aragonite biomorphic composites. *Cryst. Growth Des.* **2008**, *8*, 1515−1521.

(23) Cuéllar-Cruz, M.; Moreno, A. Synthesis of crystalline silica-carbonate biomorphs of Ba (II) under the presence of RNA and positively and negatively charged ITO electrodes: obtainment of graphite via bioreduction of CO_2 and its implications to the chemical origin of life on primitive Earth. *ACS Omega* **2020**, *5*, 5460−5469.

(24) Cuéllar-Cruz, M.; Islas, S. R.; González, G.; Moreno, A. Influence of nucleic acids on the synthesis of crystalline Ca (II), Ba (II), and Sr (II) silica-carbonate biomorphs: Implications for the chemical origin of life on primitive Earth. *Cryst. Growth Des.* **2019**, *19*, 4667−4682.

(25) Cuéllar-Cruz, M.; Moreno, A. The role of calcium and strontium as the most dominant elements during combinations of different alkaline Earth metals in the synthesis of crystalline silica-carbonate biomorphs. *Crystals* **2019**, *9*, 381.

(26) Cuéllar-Cruz, M.; Scheneider, D. K.; Stojanoff, V.; Islas, S. R.; Sánchez-Puig, N.; Arreguín-Espinosa, R.; Delgado, J. M.; Moreno, A. Formation of crystalline silica-carbonate biomorphs of alkaline Earth metals (Ca, Ba, Sr) from ambient to low temperatures: chemical implications during the primitive Earth's life. *Cryst. Growth Des.* **2020**, *20*, 1186−1195.

(27) Weiner, S. Biomineralization: A structural perspective. *J. Struct. Biol.* **2008**, *163*, 229−234.

(28) Kitadai, N.; Maruyama, S. Origins of building blocks of life: A review. *Geosci. Front.* **2018**, *9*, 1117−1153.

(29) Cairns-Smith, A.G.; *Seven clues to the origin of life*. Cambridge University Press, 1990. ISBN: 9780521398282.

(30) Kasting, J. F. Theoretical constraints on oxygen and carbon dioxide concentrations in the Precambrian atmosphere. *Precambrian Res.* **1987**, *34*, 205−229.

(31) Kasting, J. F.; Ackerman, T. P. Climatic consequences of very high carbon dioxide levels in the earth's early atmosphere. *Science* **1986**, *234*, 1383−1385.

(32) Moseley, H. *Non-ionising Radiation: Microwaves, Ultraviolet and Laser Radiation, Medical Physics Handbook*; 1st edition, Bristol Adam Hilger, 1988, *18*, 110−154.

(33) Nikafshar, S.; Zabihi, O.; Ahmadi, M.; Mirmohseni, A.; Taseidifar, M.; Naebe, M. The effects of UV Light on the chemical

and mechanical properties of a transparent Epoxy-Diamine system in the presence of an organic UV absorber. *Materials* **2017**, *10*, 180.
(34) *Solar and Ultraviolet radiation*. Radiation. Volume 100 D. Available online: https://www.ncbi.nlm.nih.gov/books/NBK304366/.
(35) IARC Working Group on the Evaluation of Carcinogenic Risks to Humans. Solar and ultraviolet radiation. In *Radiation*. International Agency for Research on Cancer, 2012.
(36) Oparin, A. I. *The origin of life, transl. A. Synge, in J. D. BernaI (1967), The Origin of Life*, Oxford University Press, London. 1924, 197−234.
(37) Oparin, A.I. *The origin of life on the Earth*, transl. A. Synge, Longmans, Edinburgh, 1957, Ch. 6.
(38) Urey, H. On the early chemical history of the Earth and the origin of life. *Proc. Natl. Acad. Sci. U. S. A.* **1952**, *38*, 351−363.
(39) Miller, S. L. A production of amino acids under possible primitive Earth conditions. *Science* **1953**, *117*, 528−529.
(40) Sarker, P. K.; Takahashi, J. I.; Obayashi, Y.; Kaneko, T.; Kobayashi, K. Photo-alteration of hydantoins against UV light and its relevance to prebiotic chemistry. *Adv. Space Res.* **2013**, *51*, 2235−2240.
(41) Kakani, V. G.; Reddy, K. R.; Zhao, D.; Sailaja, K. Field crop responses to ultraviolet-B radiation: a review. *Agric. For. Meteorol.* **2003**, *120*, 191−218.
(42) Tevini, M.; Teramura, A. H. UV-B effects on terrestrial plants. *Photochem. Photobiol.* **1989**, *50*, 479−487.
(43) Searles, P. S.; Caldwell, M. M.; Winter, K. The response of five tropical dicotyledon species to solar ultraviolet-B radiation. *Am. J. Bot.* **1995**, *82*, 445−453.
(44) Yuan, L.; Ming, Y.; Xunling, W. Effects of enhanced ultraviolet-B radiation on crop structure, growth and yield components of spring wheat under field conditions. *Field Crops Res.* **1998**, *57*, 253−263.
(45) Carteret, C.; Dandeu, A.; Moussaoui, S.; Muhr, H.; Humbert, B.; Plasari, E. Polymorphism studied by lattice phonon Raman spectroscopy and statistical mixture analysis method. Application to calcium carbonate polymorphs during batch crystallization. *Cryst. Growth Des.* **2009**, *9*, 807−812.
(46) Colagar, A. H.; Chaichi, M. J.; Khadjvand, T. Fourier transform infrared microspectroscopy as a diagnostic tool for distinguishing between normal and malignant human gastric tissue. *J. Biosci.* **2011**, *36*, 669−677.
(47) Walker, A. M.; Yu, P.; Christensen, C. R.; Christensen, D. A.; McKinnon, J. J. Fourier transform infrared microspectroscopic analysis of the effects of cereal type and variety within a type of grain on structural makeup in relation to rumen degradation kinetics. *J. Agric. Food Chem.* **2009**, *57*, 6871−6878.
(48) Buzgar, N.; Apopei, A. I. The Raman study on certain carbonates. *An. Stiint. Univ. "Al. I. Cuza" Iasi* **2009**, *55*, 97−112.
(49) Lin, C. C.; Liu, L. G. High-pressure Raman spectroscopic study of post-aragonite phase transition in witherite ($BaCO_3$). *Eur. J. Mineral.* **1997**, *9*, 785−792.
(50) Sreedhar, B.; Vani, C. S.; Devi, D. K.; Rao, M. V. B.; Rambabu, C. Shape controlled synthesis of barium carbonate microclusters and nanocrystallites using natural polysachharide—gum acacia. *Am. J. Mater. Sci.* **2012**, *2*, 5−13.
(51) Robert, F.; Chaussidon, M. A palaeotemperature curve for the Precambrian oceans based on silicon isotopes in cherts. *Nature* **2006**, *443*, 969−972.
(52) Miller, S. L.; Lazcano, A. The origin of life—did it occur at high temperatures? *J. Mol. Evol.* **1995**, *41*, 689−692.
(53) Lazcano, A.; Miller, S. L. The origin and early evolution of life: prebiotic chemistry, the pre-RNA world and time. *Cell* **1996**, *85*, 793−798.
(54) Rasmussen, B. Filamentous microfossils in a 3,235-million-year-old volcanogenic massive sulphide deposit. *Nature* **2000**, *405*, 676−679.
(55) Zhang, G.; Verdugo-Escamilla, C.; Choquesillo-Lazarte, D.; García-Ruiz, J. M. Thermal assisted self-organization of calcium carbonate. *Nat. Commun.* **2018**, *9*, 5221.
(56) Hedges, S. B.; Blair, J. E.; Venturi, M. L.; Shoe, J. L. A molecular timescale of eukaryote evolution and the rise of complex multicellular life. *BMC Evol. Biol.* **2004**, *4*, 2.
(57) Heckman, D. S.; Geiser, D. M.; Eidell, B. R.; Stauffer, R. L.; Kardos, N. L.; Hedges, S. B. Molecular evidence for the early colonization of land by fungi and plants. *Science* **2001**, *293*, 1129−1133.
(58) Rubey, W. W. Geologic history of sea water: an attempt to state the problem. *Geol. Soc. Am. Bull.* **1951**, *62*, 1111−1148.
(59) Rubey, W. W. Development of the hydrosphere and atmosphere, with special reference to probable composition of the early atmosphere. *GSA Spec. Pap.* **1955**, *62*, 631−660.
(60) Trendal, A. P. Carbon dioxide in the Precambrian atmosphere. *Geochim. Cosmochim. Acta* **1966**, *30*, 435−437.
(61) Urey, H.C. *The atmpspheres of the planets*. Handbuch der Physik, Springer-Verlag Berlin Heidelberg. 1959.
(62) Hutchinson, G.E. The biochemistry of the terrestrial atmosphere. In: *The Earth as a Planet*. G.P. Kuiper. Chicago University of Chicago Press. 1954**.**
(63) Levenspiel, O.; Fitzgerals, T. J.; Pettit, D. Earth's atmosphere before the age of dinosaurs. *Chem. Innovation* **2000**, *30*, 50−55.
(64) Lu, Z.; Chang, Y. C.; Yin, Q.-Z.; Ng, C. Y.; Jackson, W. M. Evidence for direct molecular oxygen production in CO_2 photodissociation. *Science* **2014**, *346*, 61−64.
(65) Jickells, T. D.; An, Z. S.; Andersen, K. K.; Baker, A. R.; Bergametti, G.; Brooks, N.; Cao, J. J.; Boyd, P. W.; Duce, R. A.; Hunter, K. A.; Kawahata, H.; Kubilay, N.; Laroche, J.; Liss, P. S.; Mahowald, N.; Prospero, J. M.; Ridgwell, A. J.; Tegen, I.; Torres, R. Global iron connections between desert dust, ocean biogeochemistry, and climate. *Science* **2005**, *308*, 67−71.
(66) De Faria, D. L. A.; Venâncio Silva, S.; De Oliveira, M. T. Raman microspectroscopy of some iron oxides and oxyhydroxides. *J. Raman Spectrosc.* **1997**, *28*, 873−878.
(67) Langille, D. B.; O'Shea, D. C. Raman spectroscopy studies of antiferromagnetic $FeCO_3$ and related carbonates. *J. Phys. Chem. Solids* **1977**, *38*, 1161−1171.
(68) Monika, H. Raman spectroscopy of iron oxides and (oxy)hydroxides at low laser power and possible applications in environmental magnetic studies. *Geophys. J. Int.* **2009**, *177*, 941−948.
(69) Thibeau, R. J.; Brown, C. W.; Heidersbach, R. H. Raman Spectra of Possible Corrosion Products of Iron. *Appl. Spectrosc.* **1978**, *32*, 532−535.
(70) Kiss, M. L.; Chirita, M.; Banica, R.; Ieta, A.; Savii, C.; Grozescu, I. Transition from single crystalline $FeCO_3$ to layered and ordered nanostructured α-Fe_2O_3. *Mater. Lett.* **2015**, *158*, 214−217.
(71) Vasilyeva, L. V. *Stella*, a new genus of soil Prosthecobacteria, with proposals for *Stella humosa* sp. nov. and *Stella vacuolata* sp. Nov. *Int. J. Syst. Evol. Microbiol.* **1985**, *35*, 518−521.
(72) Rye, R.; Kuo, P. H.; Holland, H. D. Atmospheric carbon dioxide concentrations before 2.2 billion years ago. *Nature* **1995**, *378*, 603−605.
(73) Pandey, A.; Bringel, F.; Meyer, J. M. Iron requirement and search for siderophores in lactic acid bacteria. *Appl. Microbiol. Biotechnol.* **1994**, *40*, 735−739.
(74) Wandersman, C.; Delepelaire, P. Bacterial iron sources: from siderophores to hemophores. *Annu. Rev. Microbiol.* **2004**, *58*, 611−647.
(75) Andrews, S. C. Iron storage in bacteria. *Adv. Microb. Physiol.* **1998**, *40*, 281−351.
(76) Briat, J. F.; Duc, C.; Ravet, K.; Gaymard, F. Ferritins and iron storage in plants. *Biochim. Biophys. Acta, Gen. Subj.* **2010**, *1800*, 806−814.
(77) Powell, A. K. Ferritin: Its mineralization. In *Metal Ions in Biological Systems: Iron Transport and Storage in Microorganisms, Plants and Animals*. Sigel, A.; Sigel, H. (eds). Dekker; New York. 1998, 515−561.
(78) Fleming, R. E.; Bacon, B. R. Orchestration of iron homeostasis. *N. Engl. J. Med.* **2005**, *352*, 1741−1744.

https://doi.org/10.1021/acsomega.1c05415
ACS Omega 2021, 6, 35629−35640

(79) Miret, S.; Simpson, R. J.; McKie, A. T. Physiology and molecular biology of dietary iron absorption. *Annu. Rev. Nutr.* **2003**, *23*, 283−301.
(80) Neilands, J. B. Siderophores: structure and function of microbial iron transport compounds. *J. Biol. Chem.* **1995**, *270*, 26723−26726.
(81) Dybas, M.; Tatara, G.; Criddle, C. S. Localization of carbon tetrachloride transformation activity of *Pseudomonas* sp strain KC. *Appl. Environ. Microbiol.* **1995**, *61*, 758−762.
(82) Jurkevitch, E.; Chen, Y.; Hadar, Y. Involvement of bacterial siderophores in the remedy of lime−induced chlorosis in peanut. *Soil Sci. Soc. Am. J.* **1988**, *52*, 1032−1037.
(83) Wang, Y.; Brown, H. N.; Crowley, D. E.; Szaniszlo, P. J. Evidence for direct utilization of a siderophore, ferrioxamine B, in axenically grown cucumber. *Plant, Cell Environ.* **1993**, *16*, 579−585.
(84) Yehuda, Z.; Shenker, M.; Hadar, Y.; Chen, Y. Remedy of chlorosis induced by iron deficiency in plants with the fungal siderophore rhizoferrin. *J. Plant Nutr.* **2000**, *23*, 1991−2006.
(85) Noorduin, W. L.; Grinthal, A.; Mahadevan, L.; Aiznberg, J. Rationally Designed Complex, Hierarchical Microarchitectures. *Science* **2013**, *340*, 832−837.

https://doi.org/10.1021/acsomega.1c05415
ACS Omega 2021, 6, 35629−35640